Sensitivity Comparison of a Self-Standing Porous Silicon Membrane Under Flow-Through and Flow-Over Conditions

David Martín-Sánchez, Salvador Ponce-Alcántara, and Jaime García-Rupérez, *Senior Member, IEEE*

***Abstract*— An optical sensor based on a self-standing porous silicon (PS) membrane is presented. The sensor was created by electrochemically etching a heavily doped p-type silicon wafer with an organic electrolyte that contained dimethylformamide. After fabrication, a high-current density close to electropolishing was applied in order to allow the detachment from the substrate using a lift-off method. The PS membrane was integrated in a microfluidic cell for sensing purposes, and reflectance spectra were continuously obtained while the target substance was flowed. A comparison of the bulk sensitivity is achieved when flowing through and over the pores is reported. During the experiments, a maximum sensitivity of 770 nm/RIU measured at 1700 nm was achieved. Experimental sensitivity values are in good agreement with the theoretical calculations performed when flowing through the PS membrane, it means that the highest possible sensitivity of that sensor was achieved. In contrast, a drop in the sensitivity of around 25% was observed when flowing over the PS membrane.**

***Index Terms*— Dimethylformamide, flow-through, lift-off, porous membrane, porous silicon, self-standing, sensing.**

I. Introduction

POROUS silicon (PS) [1] is a good material for fabricating high sensitivity optical sensors. Its porous structure is very adequate for detecting changes of the medium filling the pores since the effective refractive index of the PS film is a function of both the refractive index of the silicon (Si) and the one of the medium filling the pores [2], [3]. It is also very efficient for tasks such as biorecognition, as the available surface is larger in PS than in other sensors due to the extremely high ratio between surface and volume [4]. These features allow the miniaturization of the sensor, the reduction of its cost, as well as a faster response.

Formation of PS occurs under anodization of silicon in hydrofluoric acid (HF) solutions, known as electrochemical etching [5]. The growth of the pores is a combination of two chemical reactions: a direct dissolution of Si in fluoride and an oxidation of Si in the presence of oxygen and its later dissolution [6]. Initially, both reactions occur randomly over the Si surface but, once the holes are initially created, the electrical charges are attracted to their tips and the pores start growing in a vertical manner. As the reactions occur almost exclusively at the pore tip, changes in the anodization conditions during the etching will not affect the PS already formed, which allows the formation of layers with different porosities and thicknesses throughout the structure.

Both reactions are strongly dependent on the chemical and electrical conditions of the etching process. For instance, anodization current, electrolyte composition or wafer resistivity, define the porosity of the PS layer. The higher the current applied, the higher the porosity. On the contrary, the porosity decreases as the HF concentration in the solution increases. Additionally, the doping of the Si wafer is related to the pore density [7]. Other parameters that can be tuned during the electrochemical etching are the thickness of the PS layer, by controlling the etching time, and the pore diameter, which can range from less than 5 nm (micropores) up to more than 1 μm (macropores) [8]. However, higher sensitivities are reached for small pore sizes [9].

P-type Si wafers have some advantages concerning PS formation, e.g. better surface and vertical uniformity [10], linear etching rates [11], [12], and no need for backside illumination [7]. For heavily doped p-type Si, micropores are formed with most HF solutions [8]. However, certain applications in which pore walls are going to be biofunctionalized [13], [14] or some molecules must penetrate the pores [15] require a bigger pore diameter. For this purpose, some organic solvents, such as dimethylformamide (DMF), are combined with HF to increase the pore size during anodization [16], [17].

PS structures used for sensing purposes e.g., Fabry-Pèrot interferometers [18], distributed Bragg reflectors [19], and microcavities [20] have reported good results. Nonetheless, they may suffer some negative effects like air entrapment and bad flow diffusion that are responsible of a decrease in the sensitivity and threaten performance [21], [22]. It has been demonstrated that flowing through PS films reduces the time of detection, optimizes the sensitivity, and avoids mixture of different substances [23]. There are several methods for obtaining PS films but lift-off is the easiest and fastest way [24]. In this method, the PS structure is detached from the substrate in a single step by electrochemically etching with a current close to electropolishing. The self-standing PS membrane can be then integrated into a microfluidic cell in order to perform sensing experiments.

Manuscript received December 14, 2018; accepted January 15, 2019. Date of publication January 21, 2019; date of current version April 5, 2019. This work was supported by the Ministry of Economy and Competitiveness. The associate editor coordinating the review of this paper and approving it for publication was Prof. Aime Lay-Ekuakille. *(Corresponding author: Jaime García-Rupérez.)*

The authors are with the Nanophotonics Technology Center, Universitat Politècnica de València, 46022 Valencia, Spain (e-mail: jaigarru@ntc.upv.es).

Digital Object Identifier 10.1109/JSEN.2019.2893885

In this work, we report a comparison of sensitivities of a self-standing PS microcavity sensor when flowing different substances through and over it. The PS membrane was etched with an organic electrolyte and then detached from the Si substrate by lift-off. We have confirmed that a higher sensitivity is obtained for the same PS membrane sensing structure when the target substance is forced to pass through the pores. The sensitivity obtained when flowing through the PS membrane perfectly matches the one obtained in theoretical calculations, confirming that a complete filling of the sensor is accomplished, unlike when the flow is driven over the PS sensing membrane.

II. Materials and Methods

PS was prepared by electrochemical etching highly doped p-type Si (boron doped, ⟨100⟩ oriented, 0.01-0.02 Ω·cm resistivity) purchased from MicroChemicals GmbH (Germany). Ethanol (EtOH) and 2-Propanol (IPA) were obtained from Scharlab S.L. (Spain), and N,N-Dimethylformamide (DMF) from Sigma-Aldrich (USA). HF (48% solution in water), Hydrogen Peroxide (H_2O_2), and Sulfuric acid (H_2SO_4) were purchased from BASF (Germany). Deionized water (DIW) was produced in house by a Millipore water purification system.

All silicon samples were pre-treated for 30 min in a 3:1 volumetric mixture of H_2SO_4 and H_2O_2 for cleaning organic residues off the substrate. Afterward, they were dipped into a solution of <5% HF for 30 s to remove the native SiO_2 layer.

PS microcavity films were fabricated under galvanostatic conditions with a platinum (Pt) electrode using an electrolyte solution of HF:DIW:DMF in a 1:1:4 volumetric ratio. A multilayer structure of 12 periods was formed alternating regions of high (H) and low (L) porosity, with a defect layer in the middle of the structure in order to obtain a resonant peak within the photonic bandgap (PBG).

Since higher porosities lead to higher sensitivities, the H and L regions were designed to have 82 % and 62 % of porosity, respectively. The Looyenga model for the effective medium approximation [3] was used to calculate the refractive index from those porosity values. Furthermore, the theoretical thicknesses were calculated to satisfy the Bragg's law:

$$m\lambda/2 = nh \tag{1}$$

where m is an integer, n the refractive index, h the thickness, nh the optical thickness and λ the wavelength where the maximum light is reflected. An optimum PBG is obtained when the optical thickness of the H layer and the one of the L layer are equal to a quarter of the wavelength of the resonant peak [25].

Two different sets of structures were fabricated i.e. one to be used in the visible (VIS) region of the spectrum (500 to 800 nm) and another one for the near infrared (NIR) range (1100 to 1800 nm). The calculated thicknesses of the former were 218 nm and 163 nm, for the H and L layers, respectively. The thicknesses for the latter were 347 nm and 261 nm. A defect layer was placed in the middle of the structure by forming 6 periods of H and L layers and then 6 periods of L and H layers, meaning that the central microcavity consists of an L layer of twice its nominal thickness. Thus, the theoretical thicknesses of the whole sensor were 4572 nm and 7296 nm for the structures used in the VIS and NIR regions, respectively.

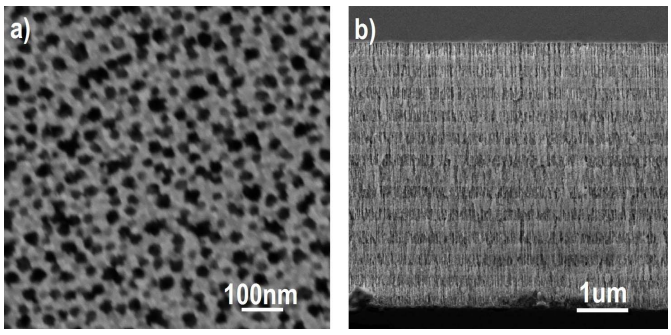

Fig. 1. FESEM images taken of (a) the PS surface, and (b) the PS section of a sample used in the VIS range. The average pore diameter measured on the surface is 30 nm. Note that those regions with a lower proportion of Si (higher porosities) are displayed in the images as darker areas.

In both set of samples, the regions of H and L porosities were formed using anodization current densities of 22 mA/cm^2 and 8 mA/cm^2, respectively. For the VIS structure, the etching times were 12 s and 19 s for the H and L layers, respectively, and 38 s for the defect layer. For the NIR structure, H and L layers were etched for 20 s and 30 s, and the defect layer for 60 s.

After the formation of all the periods comprising the PS structure, an anodization current of 45 mA/cm^2, close to electropolishing, was applied during 15 s to allow a later detachment of the PS film from the substrate. Then, the samples were oxidized in a furnace at 800 °C for 15 min in oxygen atmosphere.

Field emission scanning electron microscopy (FESEM) images were obtained for the characterization of the PS layers, using a Zeiss Ultra 55 microscope (see Fig. 1). Physical parameters were statistically determined with ImageJ processing software [26].

A microfluidic flow cell was designed for sensing with the PS film while flowing both over and through the pores. First, the membranes were detached from the substrate using a PDMS layer with holes for the tubes that had already been assembled. A microchannel was then attached between the PS film and a glass slide. Fig. 2 shows a flowchart of the whole fabrication process.

The configuration of the microfluidic cell forced the substances to pass through the PS film in those areas where the inlet and the outlet were placed, as it is depicted in Fig. 3. In this flow-through condition, the fluid filled entirely the pores. However, once the substances were in the fluidic microchannel, they were not forced to flow through the PS film. In this so-called flow-over condition, the pores were not completely filled. Therefore, by using this microfluidic configuration, both fluidic conditions were compared measuring the sensor in these two different points. An illustration of the microfluidic cell and the flow-through and flow-over areas is shown in Fig. 3.

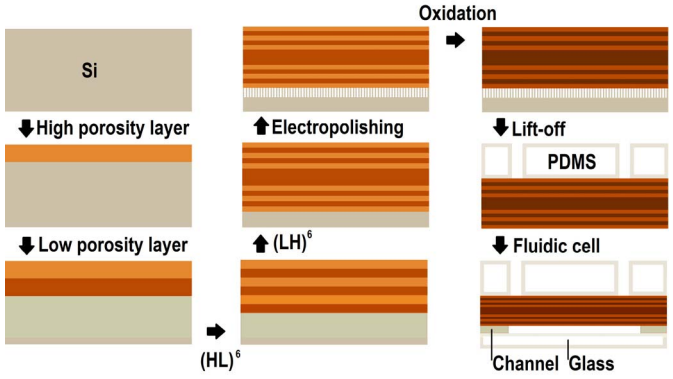

Fig. 2. Flowchart of the fabrication process for obtaining the PS films. For the samples attached to the substrate, the "electropolishing" and "lift-off" steps are omitted.

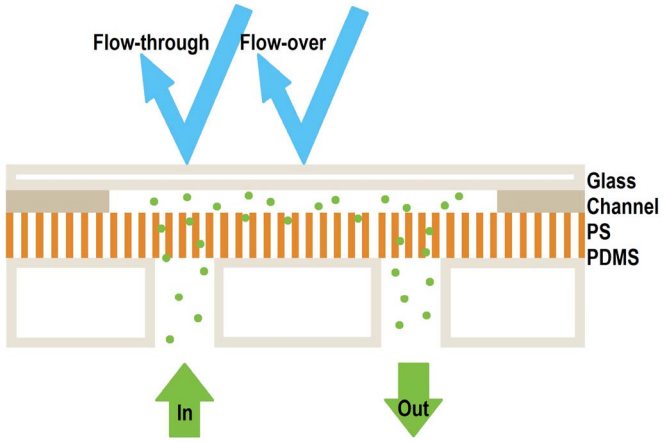

Fig. 3. Schematic view of the PS film detached from the substrate and integrated in the microfluidic cell. The flow path is illustrated with green dots. The blue arrows represent the places where flow-through and flow-over conditions can be measured.

In order to compare the performance of the PS membrane sensors, we used PS structures still attached to the Si substrate as reference sensors. These reference PS structures had identical features to the sets of samples for VIS and NIR. The fabrication process was the same except for the anodization step performed at the end of the PS etching process, which was skipped. Furthermore, as there was no need of PDMS for detaching the PS film, this step was also omitted and the inlet and outlet were placed directly on the glass of the flow cell. Fig. 4 illustrates the fluidic configuration for this set of PS reference samples. The reference sensors only worked under the flow-over condition.

During the experiments, the reflectance spectrum was recorded in order to sense the different substances. All measurements were performed using a Fourier-Transform Infrared Spectroscopy (FTIR) system (Bruker, USA) measuring in the range between 500 nm and 2500 nm. Reflectance spectra of the PS films were collected every 30 s with an acquisition time of 20 s. For the experiments, three different liquids were flowed, i.e., DIW, EtOH, and IPA. Recorded data was processed with a MATLAB (vR2016b) program and the shift

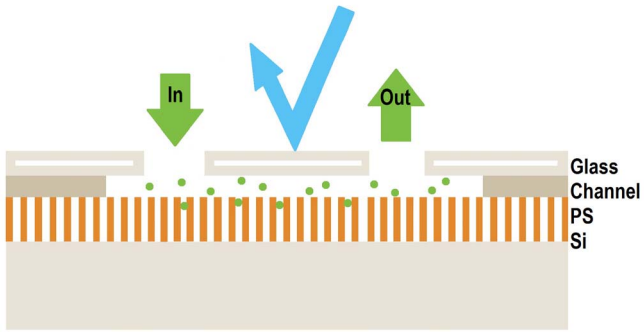

Fig. 4. Schematic view of the PS structure attached to the substrate together with the microfluidic cell. The flow path is illustrated with green dots. The blue arrow represents the place where reflectance was measured. Note that the inlet and outlet are placed in the glass instead of in the PDMS (which is not used in this setup).

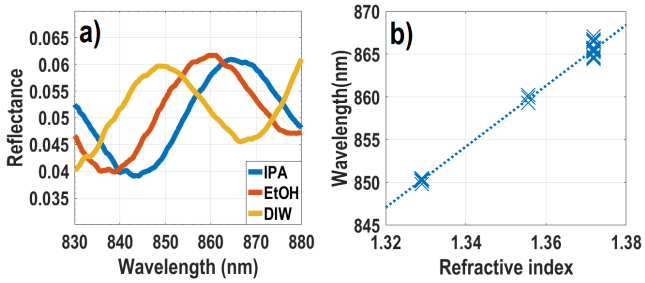

Fig. 5. (a) Example of measured reflectance spectra of the PS membrane in (yellow) DIW, (red) EtOH, and (blue) IPA. (b) Dispersion of all recorded local maxima during the experiment (crosses) and linear regression (line).

of a local maximum was measured. A Savitzky-Golay smoothing filter [27] was used for noise reduction prior to the peak search.

Sensitivity, described as the spectral shift divided by the refractive index variation, was calculated considering the refractive index of DIW, EtOH, and IPA available in the references [28], [29].

III. Results and Discussion

A shift of the reflectance spectrum towards higher wavelengths was observed due to the refractive index increase when the substance filling the pores was changed from DIW to EtOH and/or IPA. Fig. 5 (a) shows an example of how a local maximum shifts for the different fluids used. During the experiment, every substance was flowed alternately three times for 5 minutes in order to analyze the precision of the measurement.

All recorded data of each experiment were processed in order to obtain the position of a local maximum as the different substances were flowed and it was plotted versus the refractive index of the medium, as shown in Fig. 5 (b). Regression of the scatter graph was computed to obtain a linear fitting of the response of the sensor, the slope of which indicates the sensitivity to refractive index variations. Finally, the former analysis was repeated for different local maxima to acquire the sensitivity value at different wavelengths.

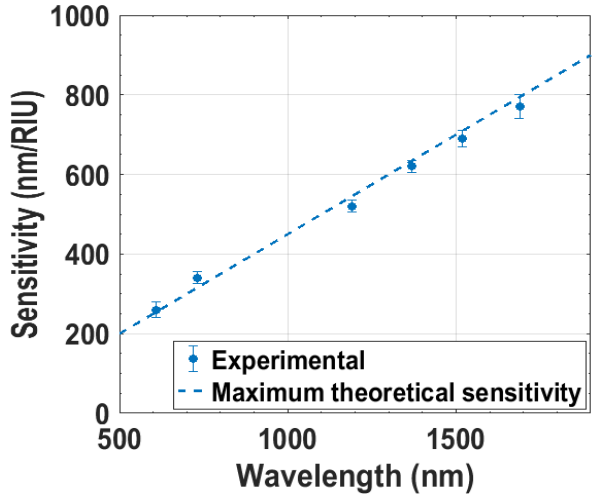

Fig. 6. Experimental sensitivity (dots) flowing through the pores and maximum theoretical sensitivity (dash line).

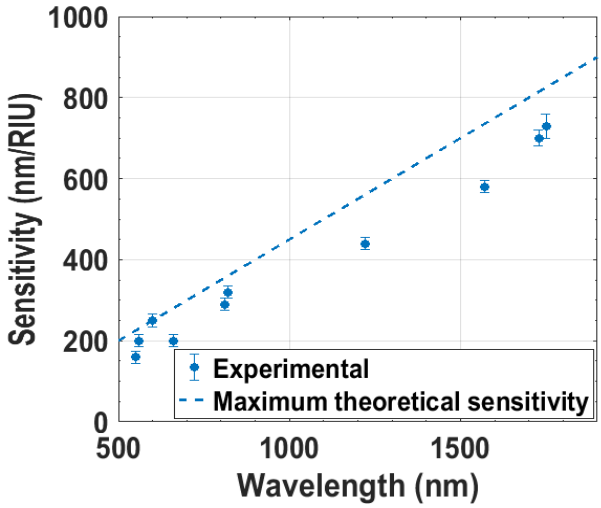

Fig. 7. Experimental sensitivity (dots) and maximum theoretical sensitivity (dash line) under flow-over conditions.

A simulation program based on the Transfer Matrix Method (TMM) [30] was used to compare the theoretical response of the PS films with the experimental one of the fabricated sensors. Thicknesses of the layers were extracted from FESEM images and porosities from fitting the reflectance measurements by means of the least-squares method.

The set of samples designed for the VIS range of the spectrum was estimated to have 230 and 170 ± 5 nm of thickness and 82 and 62 ± 2 % of porosity for the H and L layers, respectively. In the case of the samples used in the NIR, the estimated values of the thicknesses were 360 and 270 ± 5 nm, respectively, while the porosities remained the same. Our calculations determined that the theoretical sensitivity of the sensors linearly varies from 200 to 900 nm/RIU in the range of 500-1900 nm (dashed line in Fig. 5 to 7), considering that the pores of the PS layers were filled completely.

Fig. 6 shows the experimental sensitivity in the range from 600 to 1700 nm obtained after measuring the spectrum shift when flowing through the PS membrane. For each experiment, there is an average value of the sensitivity at certain wavelength (a dot in Fig. 6). The associated error was calculated as the standard error of the mean, taking into account all the recorded measurements (plotted as an error bar in Fig. 6), and it is different for each experiment. The achieved sensitivity in that region of the spectrum ranged between 260 ± 10 and 770 ± 20 nm/RIU.

Experimental results were found to be in nearly perfect agreement with the theoretical calculations, meaning that the highest possible sensitivity of the sensor was achieved by flowing through the pores.

The design of the microfluidic cell also allowed us to carry out another series of measurements with the same samples on a region where liquids were not forced to flow through the pores but over them (see Fig. 3). Experimental sensitivity is shown in Fig. 7. A sensitivity between 160 ± 10 and 730 ± 20 nm/RIU was achieved for wavelengths between 550 and 1750 nm.

In this case, when we stopped forcing the liquids to pass through the pores, the sensitivity dropped. Our results show

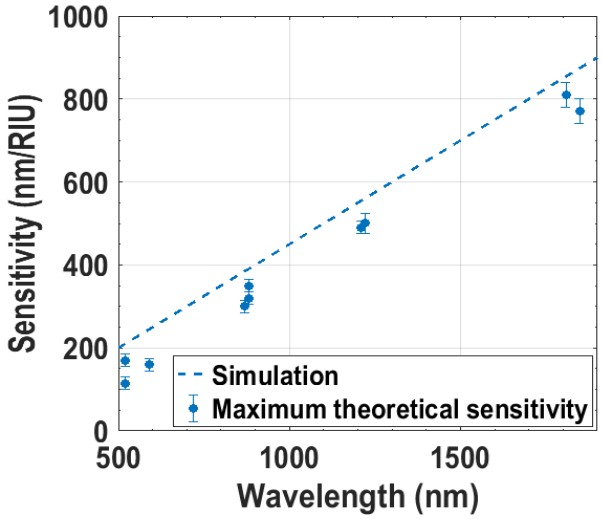

Fig. 8. Experimental sensitivity (dots) flowing over the pores of the reference sensor and simulated response (dash line).

that a reduction of about 20-30 % must be expected when doing so. This means that the sensor was not entirely filled with the target substance, whether mixed with the previous medium or with the air that originally filled the pores, and consequently the effective refractive index was lower than the effective refractive index calculated for maximum sensitivity conditions. Moreover, the reduction was not consistent across several experiments and thus the sensitivity cannot be predicted when flowing-over the PS membrane.

A similar experiment was carried out with the reference set of samples where the PS film was still attached to the substrate, with the purpose of comparing the influence of detaching the PS film. The results are summarized in Fig. 8. In the region between 500 and 1850 nm, a sensitivity between 115 ± 10 and 810 ± 20 nm/RIU was achieved. Reductions of around 20-30 % in the sensitivity have been measured again, as it happened for the detached PS membrane under flow-over

regime. We believe that the reason behind that drop lies in the resistance that liquids face when penetrating the pores rather than air entrapment.

IV. Conclusions

In this work, we have presented the fabrication of a PS membrane detached from the substrate via a lift-off method and its use as a sensor for the detection of refractive index changes. Flowing through open-ended pores optimizes the sensitivity and allows reaching the theoretical expectations. A sensitivity of 340 nm/RIU has been achieved in the visible range of the spectrum and of 770 nm/RIU in the near infrared range. A drop between 20-30% can be expected when flowing over the pores.

References

[1] C. Pacholski, "Photonic crystal sensors based on porous silicon," *Sensors*, vol. 13, no. 4, pp. 4694–4713, Apr. 2013, doi: 10.3390/s130404694.

[2] D. A. G. Bruggeman, "Berechnung verschiedener physikalischer konstanten von heterogenen substanzen. I. Dielektrizitätskonstanten und leitfähigkeiten der mischkörper aus isotropen substanzen," *Ann. Phys.*, vol. 24, no. 5, pp. 636–664, 1935, doi: 10.1002/andp.19354160705.

[3] H. Looyenga, "Dielectric constants of heterogeneous mixtures," *Physica*, vol. 31, no. 3, pp. 401–406, 1965.

[4] O. Bisi, S. Ossicini, and L. Pavesi, "Porous silicon: A quantum sponge structure for silicon based optoelectronics," *Surf. Sci. Rep.*, vol. 38, nos. 1–3, pp. 6–21, 2000.

[5] K. W. Kolasinski, "Etching of silicon in fluoride solutions," *Surf. Sci.*, vol. 603, nos. 10–12, pp. 1904–1911, Jun. 2009, doi: 10.1016/j.susc.2008.08.031.

[6] M. J. Sailor, "Fundamentals of porous silicon preparation," in *Porous Silicon in Practice: Preparation, Characterization and Applications*, 1st ed. Hoboken, NJ, USA: Wiley, 2012, pp. 1–43.

[7] H. Föll, M. Christophersen, J. Carstensen, and G. Hasse, "Formation and application of porous silicon," *Mater. Sci. Eng. R, Rep.*, vol. 39, no. 4, pp. 93–141, Nov. 2002.

[8] G. X. Zhang, "Porous silicon: Morphology and formation mechanisms," in *Modern Aspects of Electrochemistry*, vol. 39, C. Vayenas and M. E. Gamboa-Adelco, Eds. Boston, MA, USA: Springer, 2006, ch. 2, pp. 65–133, doi: 10.1007/978-0-387-31701-4_2.

[9] I. Suárez, V. Chirvony, D. Hill, and J. Martínez-Pastor, "Simulation of surface-modified porous silicon photonic crystals for biosensing applications," *Photon. Nanostruct. Fundam. Appl.*, vol. 10, no. 3, pp. 304–311, Jun. 2012, doi: 10.1016/j.photonics.2011.04.014.

[10] V. Agarwal, "Porous silicon multilayers and superlattices," in *Handbook of Porous Silicon*, L. T. Canham, Ed. Cham, Switzerland: Springer, 2014, pp. 153–162.

[11] A. Halimaoui, "Porous silicon formation by anodization," in *Properties of Porous Silicon*, vol. 12, L. T. Canham, Ed. London, U.K.: The Institution of Electrical Engineers, 1997.

[12] M. G. Berger, M. Thönissen, C. Dieker, L. Vescan, H. Münder, and H. Lüth, "Formation techniques for porous silicon superlattices," *Thin Solid Films*, vol. 255, nos. 1–2, pp. 59–62, Jan. 1995, doi: 10.1016/0040-6090(94)05604-C.

[13] S. Mariani, L. M. Strambini, and G. Barillaro, "Femtomole detection of proteins using a label-free nanostructured porous silicon interferometer for perspective ultrasensitive biosensing," *Anal. Chem.*, vol. 88, no. 17, pp. 8502–8509, Sep. 2016, doi: 10.1021/acs.analchem.6b01228.

[14] M. Arroyo-Hernandez, R. J. Martın-Palma, J. Pérez-Rigueiro, J. P. García-Ruiz, J. L. García-Fierro, and J. M. Martínez-Duart, "Biofunctionalization of surfaces of nanostructured porous silicon," *Mater. Sci. Eng. C*, vol. 23, nos. 6–8, pp. 697–701, Dec. 2003, doi: 10.1016/j.msec.2003.09.159.

[15] L. M. Karlsson, P. Tengvall, I. Lundström, and H. Arwin, "Penetration and loading of human serum albumin in porous silicon layers with different pore sizes and thicknesses," *J. Colloid Interface Sci.*, vol. 266, no. 1, pp. 40–47, 2003.

[16] V. Lehmann, R. Stengl, and A. Luigart, "On the morphology and the electrochemical formation mechanism of mesoporous silicon," *Mater. Sci. Eng. B*, vols. 69–70, pp. 11–22, Jan. 2000.

[17] S. Haldar, A. De, S. Chakraborty, S. Ghosh, and U. Ghanta, "Effect of dimethylformamide, current density and resistivity on pore geometry in p-type macroporous silicon," *Procedia Mater. Sci.*, vol. 5, pp. 764–771, Jan. 2014, doi: 10.1016/j.mspro.2014.07.326.

[18] T. Hutter, M. Horesh, and S. Ruschin, "Method for increasing reliability in gas detection based on indicator gradient in a sensor array," *Sens. Actuators B, Chem.*, vol. 152, no. 1, pp. 29–36, Feb. 2011, doi: 10.1016/j.snb.2010.09.058.

[19] A. Kovacs, A. Malisauskaite, A. Ivanov, U. Mescheder, and R. Wittig, "Optical sensing and analysis system based on porous layers," in *Proc. 17th Int. Conf. Miniaturized Syst. Chem. Life Sci.*, Freiburg, Germany, 2013, pp. 275–277.

[20] L. Pavesi, "Porous silicon dielectric multilayers and microcavities," *Riv. Nuovo Cimento*, vol. 20, no. 10, p. 1, 1997.

[21] Y. Zhao, G. Gaur, R. L. Mernaugh, P. E. Laibinis, and S. M. Weiss, "Comparative kinetic analysis of closed-ended and open-ended porous sensors," *Nanosc. Res. Lett.*, vol. 11, no.1, p. 395, 2016.

[22] N. Kumar, E. Froner, R. Guider, M. Scarpa, and P. Bettotti, "Investigation of non-specific signals in nanoporous flow-through and flow-over based sensors," *Analyst*, vol. 139, no. 6, pp. 1345–1349, 2014, doi: 10.1039/c3an01996a.

[23] Y. Zhao, G. Gaur, S. T. Retterer, P. E. Laibinis, and S. M. Weiss, "Flow-through porous silicon membranes for real-time label-free biosensing," *Anal. Chem.*, vol. 88, no. 22, pp. 10940–10948, Nov. 2016, doi: 10.1021/acs.analchem.6b02521.

[24] C. S. Solanki, R. R. Bilyalov, J. Poortmans, J.-P. Celis, J. Nijs, and R. Mertens, "Self-standing porous silicon films by one-step anodizing," *J. Electrochem. Soc.*, vol. 151, no. 5, pp. C307–C314, 2004, doi: 10.1149/1.1688797.

[25] G. Lerondel, "Optical properties of porous silicon," in *Porous Silicon: From Formation to Application*, I. G. Korotcenkov, London, U.K.: Taylor & Francis, 2016, pp. 225–244.

[26] W. S. J. Rasband, "ImageJ," U.S. Nat. Inst. Health, Bethesda, MD, USA, Tech. Rep. 1.51n, 2016. [Online]. Available: https://imagej.nih.gov/ij/

[27] A. Savitzky and M. J. E. Golay, "Smoothing and differentiation of data by simplified least squares procedures," *Anal. Chem.*, vol. 36, no. 8, pp. 1627–1639, 1964.

[28] G. M. Hale and M. R. Querry, "Optical constants of water in the 200-nm to 200-μm wavelength region," *Appl. Opt.*, vol. 12, no. 3, pp. 555–563, 1973.

[29] E. Sani and A. Dell'Oro, "Spectral optical constants of ethanol and isopropanol from ultraviolet to far infrared," *Opt. Mater.*, vol. 60, pp. 137–141, Oct. 2016, doi: 10.1016/j.optmat.2016.06.041.

[30] R. B. Balili, "Transfer matrix method in nanophotonics," *Int. J. Mod. Phys.*, vol. 17, pp. 159–168, Jan. 2012.

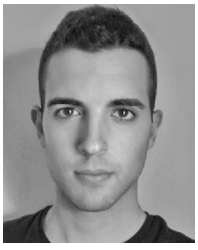

David Martín-Sánchez received the B.S. degree in telecommunication from the University of Seville, Spain, in 2014, and the M.S. degree in biomedical engineering from the Universitat Politècnica de València, Spain, in 2016, where he is currently pursuing the Ph.D. degree in telecommunication with the Nanophotonics Technology Center (NTC). Since 2016, he has been a Research Assistant with the Biophotonics Research Group, NTC. His research interests include the design, fabrication, and characterization of photonic sensors based on porous silicon.

Salvador Ponce-Alcántara received the M.S. degree in electronic engineering from the University of Granada, Spain, in 2002, and the Ph.D. degree in telecommunication from the Polytechnic University of Madrid, Spain, in 2007. In 2006, he was a Visiting Researcher with the Institute for Energy Technology, Kjeller, Norway. From 2007 to 2011, he was with the Research and Development Department, Isofotón, Málaga, and Pevafersa, Zamora, Spain. In 2011, he was with the Nanophotonics Technology Center, Universitat Politècnica de València, as a Senior Researcher, where he has been an Assistant Professor since 2015. He holds one utility model and one patent. His research interests include the simulation, characterization, and development of high sensitivity porous silicon photonic sensors.

Jaime García-Rupérez (M'03–SM'16) received the M.S. and Ph.D. degrees in telecommunication from the Universitat Politécnica de Valéncia, Spain, in 2002 and 2008, respectively. He has been an Associate Professor with the Universitat Politècnica de València since 2005 and a Leader of the Nanophotonics Technology Center, Biophotonics Research Group, since 2008. He has authored over 120 journal and conference publications, one book chapter, and holds four patents. Dr. García-Rupérez is currently the Principal Investigator of two Horizon 2020 European projects focused on the development of high-sensitivity photonic sensing devices for medical diagnosis (H2020-ICT-SAPHELY and H2020-HEALTH-PHOCNOSIS) and of one national project targeting the development of analysis systems based on porous materials for the detection of biological threats (OPTONANOSENS). His work focuses on the development of integrated photonic biosensing systems for its application in fields of medical diagnosis, environmental control, or biological safety.